PCCP

PAPER

View Article Online
View Journal | View Issue

Cite this: *Phys. Chem. Chem. Phys.*, 2017, **19**, 13182

Investigation of the push–pull effects on β-functionalized benzoporphyrins bearing an ethynylphenyl bridge†

R. G. Waruna Jinadasa, Michael B. Thomas, Yi Hu, Francis D'Souza* and Hong Wang*

A series of β-pyrrole functionalized push–pull porphyrins with amine push groups linked *via* an ethynylphenyl spacer, and cyclic imide or carboxylic esters as pull groups have been newly synthesized and characterized. The β-pyrrole functionalized ethynylphenyl spacer extends the conjugation of the porphyrin π-system, as reflected by their red-shifted absorbance and fluorescence spectra. The computed structures revealed no steric hindrance between the porphyrin π-system and the β-substituents. The calculated HOMO and LUMO of compounds **WJ2** and **WJ3** display significant segregation, where the electron density in the HOMO and LUMO is mainly located at the donor component and the acceptor component, respectively. The orbital segregation is likely attributed to the introduction of the electron-donating amine group at the porphyrin periphery. Electrochemical studies revealed the expected lower HOMO–LUMO gap as a result of the facile oxidation and reduction of the push–pull porphyrins. As a consequence of the push–pull effects, a reduction in fluorescence intensity and lifetime was observed, especially for compound **WJ3** having two electron-donating amino groups and a strongly electron-withdrawing cyclic imide group. Femtosecond transient absorption spectral studies revealed the successful formation of the singlet excited state in all of these push–pull porphyrins. Due to the occurrence of intramolecular charge transfer-type interactions, relaxation of the singlet excited state was found to be faster in compound **WJ3** compared to other two derivatives in polar solvent but not in nonpolar solvent. Such charge transfer-type interactions from the triplet excited state were also observed in the case of compound **WJ3** in benzonitrile. The present findings bring out the importance of push–pull effects in governing the ground and excited (singlet and triplet) state properties of free-base porphyrins.

Received 2nd January 2017,
Accepted 24th April 2017

DOI: 10.1039/c7cp00024c

rsc.li/pccp

Introduction

Push–pull porphyrins have been a subject of long-lasting research interest owing to their potential applications in organic electronics, opto-electronics and photonics.[1–5] In particular, push–pull porphyrins have attracted intense attention in the field of dye-sensitized solar cells (DSSCs) in recent years.[3,6–8] The introduction of a push (electron-donating) and a pull (electron-withdrawing) group at the porphyrin periphery has made a remarkable impact on the solar power conversion efficiency of porphyrin-based DSSCs, converting porphyrin sensitizers from one of the worst to the best performer in DSSCs.[9–15] Over the past few years, a new family of efficient sensitizers has been created with the push–pull strategy through enhancing directional electron flow from the sensitizer to the semiconductor.[3,7]

The majority of the push–pull porphyrins in the literature are functionalized at the porphyrin *meso*-positions.[7] β-Functionalized push–pull porphyrins have been rarely studied due to their difficult accessibility.[16–18] Functionalization of porphyrins at the β-positions is expected to have a different influence on the electronic and optical properties from that at the *meso*-positions. Stimulated by the impressive advances made in *meso*-functionalized push–pull porphyrins, we became interested in developing β-functionalized push–pull π-extended porphyrins.[19,20] In a previous study,[21] we reported a series of push–pull dibenzoporphyrins (Fig. 1), in which a variety of electron-withdrawing groups (pull group) were attached to the porphyrin β,β′-positions and the *p*-methoxy group on a phenyl bridge served as the push group. Our previous work showed that the electronic and electrochemical properties of these opp-dibenzoporphyrins (opp: the two benzene rings are fused at the opposite β,β′-positions of the

Department of Chemistry, University of North Texas, 1155 Union Circle, #305070, Denton, TX 76203-5017, USA. E-mail: Francis.DSouza@UNT.edu, hong.wang@unt.edu

† Electronic supplementary information (ESI) available: ^{1}H, ^{13}C NMR and MALDI-mass spectra of newly synthesized porphyrins, spectroelectrochemical data, and additional femto- and nanosecond transient absorption data. See DOI: 10.1039/c7cp00024c

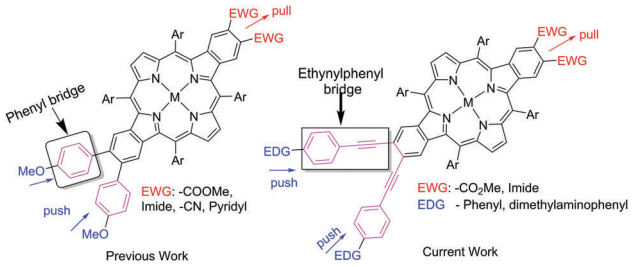

Fig. 1 β-Functionalized push–pull opp-dibenzoporphyrins.

porphyrin core) are susceptible to changes of the electron-withdrawing groups. On the other hand, the electron-donating group, *i.e. p*-methoxy group, showed a limited influence on the electronic and electrochemical properties of the porphyrins due to the restricted rotation arising from steric hindrance between the substituents and the benzoporphyrin core. In this work, we present a new series of push–pull dibenzoporphyrins, in which an ethynylphenyl spacer is inserted between the push (tertiary amine) groups and the benzoporphyrin core (Fig. 1). The inclusion of the ethynyl bridge is to release the steric stress brought by the phenyl spacer, so that the porphyrin core would be fully conjugated to the electron-donating group to enhance the electronic coupling between the push and the pull groups. The effect of both the push groups and the pull groups was investigated in this work.

Results and discussion

Molecular design and synthesis

The synthesis of dibenzoporphyrin derivatives **WJ1–WJ3** is shown in Scheme 1. All of the dibenzoporphyrin derivatives of this study were synthesized from dibromoporphyrin **1**. Monobenzoporphyrin **2** was synthesized from dibromoporphyrin **1** using a palladium catalyzed cascade reaction involving a domino Heck reaction, cyclization of alkenes and aromatization. Monobenzoporphyrin **4** bearing a cyclic imide was synthesized from monobenzoporphyrin **2**. The vicinal ester groups of compound **2** were converted into an imide by refluxing in aniline. Regioselective bromination of monobenzoporphyrins **2** and **4** with NBS produced 12,13-dibromobenzoporphyrins **3** and **5**, respectively. The coupling reaction of 12,13-dibromobenzoporphyrin **3** with an enyne using the $Pd(OAc)_2/PPh_3$ catalytic system was attempted first. However, the mono-substituted Heck product was obtained as the major product. Higher temperature and additional equivalents of the enyne resulted in major polymerization of the enyne. In order to alleviate the polymerization problem, the Heck reaction was carried out at 40 °C using $Pd[P(tBu)_3]_2$ in THF. Cyclization followed by dehydrogenation of the Heck product in refluxing THF gave monobenzoporphyrins **WJ1–WJ3** in moderate yields. All these compounds were characterized using ^1H and ^{13}C NMR spectroscopy and MALDI-LTQ-XL-Orbitrap spectrometry (see the ESI† for spectral details).

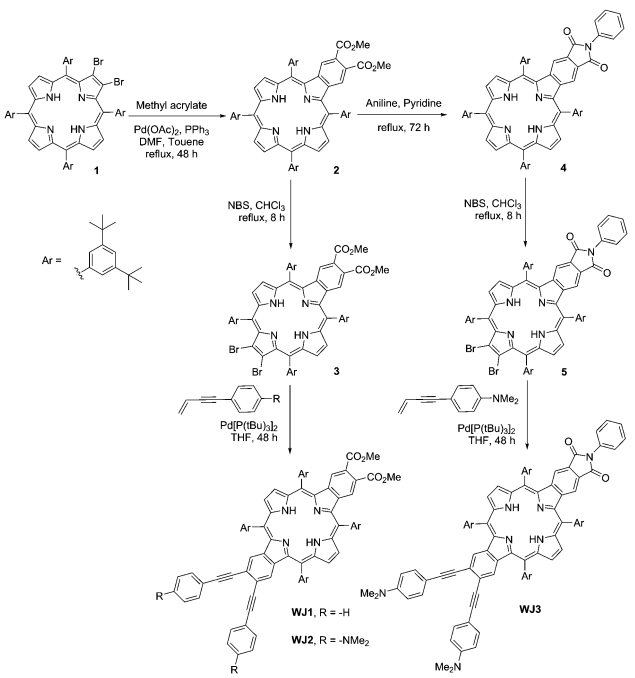

Scheme 1 Synthesis of push–pull opp-dibenzoporphyrins **WJ1–WJ3**.

Optical absorbance and fluorescence properties

Opp-dibenzoporphyrin **WJ1** bears two moderate electron-withdrawing ester groups on one fused benzene ring and two ethynylphenyl groups, which are weakly electron donating, on the other fused benzene ring at the opposite β,β′-positions of the porphyrin. In opp-dibenzoporphyrin **WJ2**, these two ester groups are converted to a cyclic imide group, which is much more strongly electron withdrawing than the ester group.

Push–pull opp-dibenzoporphyrin **WJ3** carries both strongly electron-donating amino and strongly electron-withdrawing cyclic imide groups. The UV-vis absorption spectra of **WJ1–WJ3** in benzonitrile are compiled in Fig. 2. Opp-dibenzoporphyrin **WJ1** displays a symmetrical Soret band at 452 nm and four Q bands at 533 nm, 570 nm, 612 nm and 668 nm, typical of UV-vis absorptions for symmetrical free-base porphyrins.[21] As compared with **WJ0** (Fig. 3) in the previous work,[22] the Soret band of **WJ1** is red-shifted by 5 nm, due to the inclusion of a conjugated ethynyl bridge. It is surprising that the Soret band of **WJ1** is narrower and more symmetrical than that of **WJ0**, given that the structure of **WJ1** is less symmetric than **WJ0**. The UV-vis absorption spectrum of **WJ2** shows significantly different features from those of **WJ1**. The Soret band becomes unsymmetrical with a shoulder, and is much more broadened and red-shifted by 7 nm to 459 nm. The Q bands of **WJ2** also display a different pattern from that of **WJ1**. While all of the Q bands are slightly red-shifted relative to those of **WJ1**, the Q band at 573 nm is significantly enhanced. Considering that all of these changes in the absorption spectrum of **WJ2** are simply due to the incorporation of a strongly electron-donating amino group at the *para*-position on the phenyl ring of the phenylethynyl bridge; the impact of the electron-donating group on its electronic properties is enormous. Upon concerting these two ester groups of **WJ2** to the cyclic imide group in **WJ3**, the Soret band is further red-shifted by 7 nm to 466 nm. The Q bands are all red-shifted relative to those of **WJ2** by 4–11 nm. The shoulder of the Soret

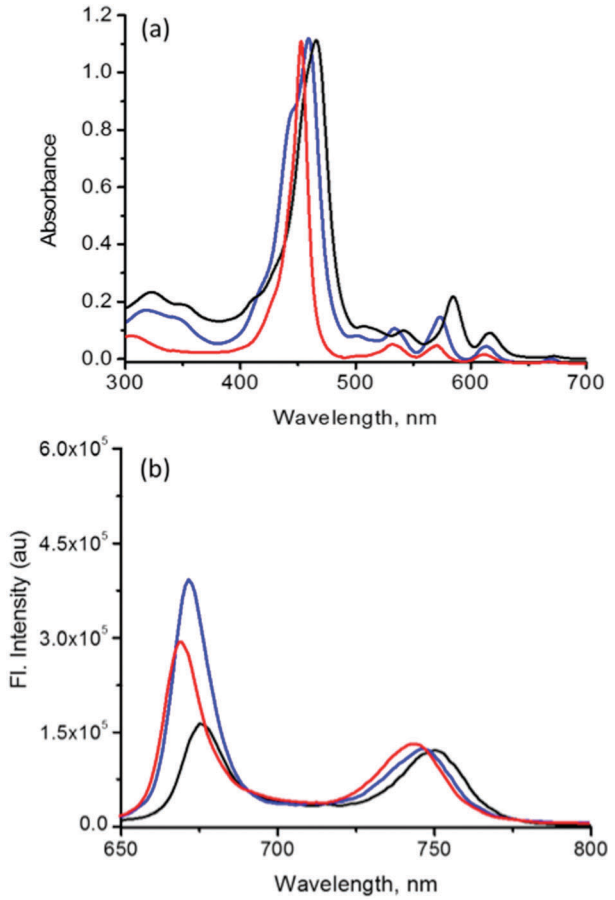

Fig. 2 (a) UV-visible absorption and (b) fluorescence spectra of **WJ1** (red), **WJ2** (blue), and **WJ3** (dark) in benzonitrile. The compounds were excited at their Soret band maxima.

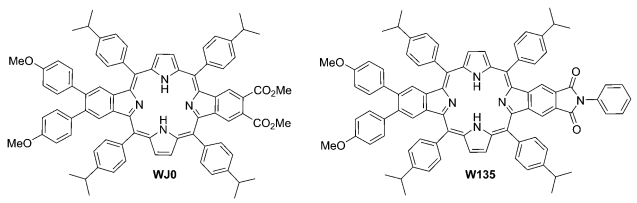

Fig. 3 The structure of push–pull opp-dibenzoporphyrins bearing a phenyl bridge between the electron-donating group and the benzoporphyrin core.

band becomes less obvious for **WJ3**, and the Q band at 584 nm is much further enhanced. These data once again illustrate the influence of the electron-withdrawing groups on the electronic properties of benzoporphyrins.

The steady-state fluorescence spectra of **WJ1–WJ3** measured in benzonitrile are shown in Fig. 2b. All these opp-dibenzoporphyrins showed two emission bands in the 670–680 nm and 740–760 nm ranges. While the 0,0 emission band located in the 670–680 nm range was much more intense than the 0,1 band in the 740–760 nm range for **WJ1** and **WJ2**, similar to that of **WJ0**, the intensity of emission at 740–760 nm is significantly reduced for **WJ3**. The fluorescence lifetimes were also measured using the time-correlated single photon counting (TCSPC) technique using nanoLED excitation sources. The decay profile could be fitted to a monoexponential decay function with lifetimes of 16.75, 16.88, and 14.51 ns for **WJ1**, **WJ2** and **WJ3**, respectively, in toluene, and 15.93, 6.54, and 2.54 ns for **WJ1**, **WJ2** and **WJ3**, respectively, in benzonitrile (see Table S1 and Fig. S3 for decay data and decay curves, ESI†). It should be pointed out here that the standard deviation of the toluene lifetime is 0.065 ns, thus the difference between 16.75 and 16.88 is not statistically significant. The reduced fluorescence lifetimes for **WJ2** and **WJ3** relative to **WJ1**, especially in polar benzonitrile suggest electron-donating and electron-withdrawing push–pull effects in the latter two compounds.

Geometry optimization and electronic structure

DFT calculations (B3LYP/6-31G(d))[23] were performed for **WJ1–WJ3** to provide insights into the electronic properties of these compounds (Fig. 4). The electron density on both the HOMO and the LUMO of **WJ1** is distributed over the porphyrin core, the two fused benzene rings and the ethynyl bridge. Both the electron-donating phenyl groups and the electron-withdrawing ester groups are not heavily involved in these frontier orbitals for **WJ1**. Upon introducing strongly electron-donating amino groups in **WJ2**, the profile of these frontier orbitals is completely changed. The electron density on the HOMO of **WJ2** is mainly shifted to the electron donating part of the molecule, involving almost no porphyrin core. On the other hand, the electron density on the LUMO of **WJ2** is primarily located at the porphyrin core. It is notable that the electron-withdrawing ester groups do not participate in the LUMO. The HOMO and LUMO of push–pull **WJ3** show a similar pattern to that of **WJ2**, except that the more strongly electron-withdrawing cyclic imide group participates in the LUMO for **WJ3**. Such orbital segregation is not observed for opp-dibenzoporphyrins bearing only strongly electron-withdrawing groups (refer to the orbitals of **W135** in Fig. 4, see the structure of **W135** in Fig. 3).[22] These data demonstrate that the electron-donating amino group plays a much more important role than the electron-withdrawing group in the HOMO/LUMO segregation. These data also show the importance of the acetylene bridge in facilitating the interaction between the electronic push and pull groups. The singly occupied molecular orbitals (SOMOs) of the investigated compounds were also investigated. As shown in

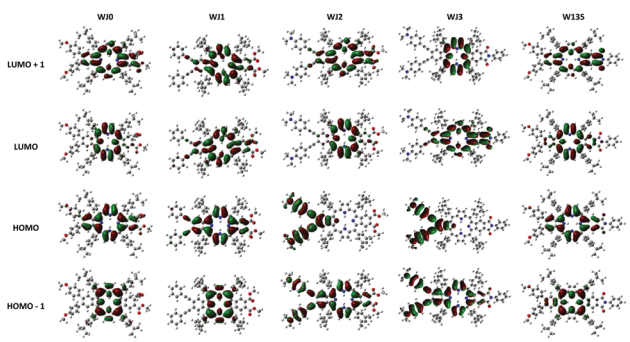

Fig. 4 Orbital isodensity surface of the HOMO and LUMO for **WJ0**, **WJ1**, **WJ2**, **WJ3**, and **W135** obtained by B3LYP/6-31G(d) level calculations.

Fig. S7 in the ESI,† all of them revealed orbital coefficients confined to the porphyrin π-system with no appreciable coefficients on either the push or pull groups, suggesting localized transitions.

Electrochemical and spectroelectrochemical studies

The electrochemical and spectroelectrochemical properties of the investigated push–pull porphyrins were investigated by differential pulse voltammetry (DPV) in benzonitrile containing 0.1 M (n-Bu_4N)ClO_4. As shown in Fig. 5, all of the compounds revealed the expected two one-electron oxidations and two one-electron reductions within the potential window of the solvent. Most of the redox processes were reversible as judged from the cyclic voltammetry studies. Compound **WJ3** with notable push–pull substituents revealed the first oxidation and reduction processes located at 0.83 and −1.10 V *vs.* Ag/AgCl, respectively, yielding an electrochemical HOMO–LUMO gap of 1.94 eV. For **WJ1** and **WJ2** having moderate push–pull groups, the HOMO–LUMO gap was found to be larger: 2.14 V for **WJ1** and 2.01 for **WJ2**. The larger HOMO–LUMO gap was due to the harder to reduce and oxidize porphyrin ring in these cases (1.0 and −1.41 V for **WJ1** and 0.84 and −1.16 V for **WJ2**). The HOMO–LUMO gaps for the current series of compounds were relatively smaller compared to those of the earlier reported series of compounds[21] due to extended π-conjugation caused by the ethynylphenyl bridges. Nonetheless, the smaller HOMO–LUMO gap due to the presence of push–pull entities directly attached to the porphyrin β-pyrrolic positions is noteworthy.

Further spectroelectrochemical studies were performed to ascertain that the redox reactions involve the porphyrin π-system and not the peripheral substituents. Fig. S4 (ESI†) shows the spectral changes observed during the first oxidation and reduction of **WJ3** in benzonitrile. During the oxidation, the Soret band revealed a blue-shift from 470 nm to 463 nm, while the visible bands revealed diminished intensity. An isosbestic point at 496 nm was also observed. These spectral changes were found to be fully reversible. During the first reduction of **WJ3**, the Soret band revealed diminished intensity with the appearance of a new band at 501 nm. In the visible region, new peaks at 625 and 698 nm were also observed. An isosbestic point at 478 nm was also observed. Similar spectral changes were observed for the other investigated free-base porphyrins. These spectral changes were typical of the porphyrin ring based oxidation and reduction processes suggesting that the peripheral electron donating and electron withdrawing groups are not directly involved.[24]

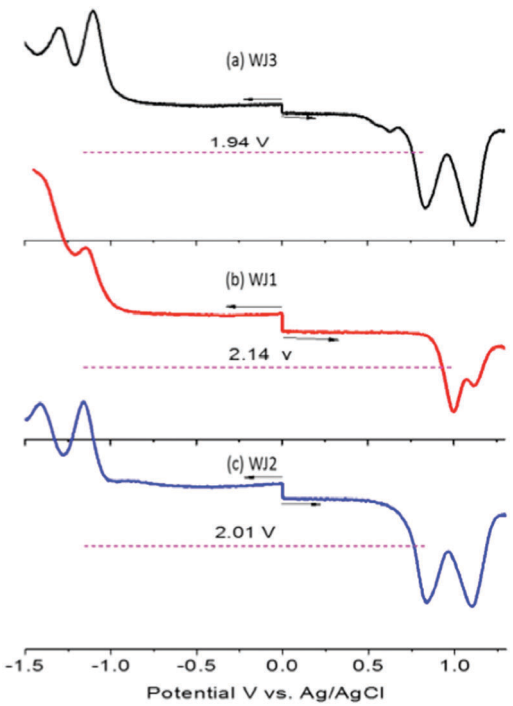

Fig. 5 Differential pulse voltammograms of the indicated compounds in benzonitrile containing 0.1 M (n-Bu_4N)ClO_4. Scan rate = 5 mV s^{-1}, pulse width = 0.25 s, pulse height = 0.025 V.

Transient absorption spectral studies

The time-resolved emission studies indicated that the lifetime of **WJ1** and **WJ2** is typical of free-base porphyrins. The lifetime of **WJ3**, however, is reduced substantially, likely due to the presence of the stronger push and pull substituents. Femtosecond transient absorption spectral studies were performed on **WJ1**, **WJ2** and **WJ3** to seek evidence of intramolecular charge transfer-type interactions enabled by the presence of electron rich and deficient substituents upon photoexcitation of these porphyrin derivatives. Two solvents, polar benzonitrile and nonpolar toluene were employed. It is expected that the polar solvent would promote intramolecular charge transfer, while such a process would be minimal in nonpolar toluene. For **WJ3** in benzonitrile, immediately after excitation (400 nm of 100 fs pulses), spectral features corresponding to the singlet excited free-base porphyrin appeared (see the spectrum recorded at 3 ps in Fig. 6a). That is, positive peaks at 495, 558, 646, and 1043 nm and negative peaks at 540, 580, 616, 675, and 750 nm were observed. The first three peaks arose from ground state depletion, while the two near-IR peaks were due to the stimulated emission of the free-base porphyrins. The 1043 nm peak has been assigned to the singlet–singlet transition of free-base porphyrins as a similar peak for zinc and aluminium porphyrins was reported earlier.[25–27] Decay of the positive peaks and recovery of the negative peaks resulted in the appearance of new and less intense peaks with maxima at 504 and 832 nm, corresponding to the triplet excited state. Fig. 6b shows the time profile of the singlet–singlet peak at 1043 nm along with those of **WJ1** and **WJ2** for comparison purpose (see Fig. S5 in the ESI† for the transient spectra of **WJ1** and **WJ2**). Decay was much faster in the case of **WJ3** compared to the other two porphyrin derivatives, and the decay persisted over 3 ns, which is consistent with the longer singlet excited lifetimes of the free-base porphyrins. Any spectral evidence pertaining to the charge transfer state, $EDG^{\delta+}$–H_2P–$EWG^{\delta-}$ was hidden under the strong absorption/stimulated emission peaks of the porphyrins.

As expected, the transient spectra recorded in toluene revealed peaks corresponding to the singlet excited porphyrin. That is, peaks corresponding to transitions from the singlet excited state, ground state bleaching and stimulated emission in the expected wavelength region were observed (see Fig. 6c). The decay time

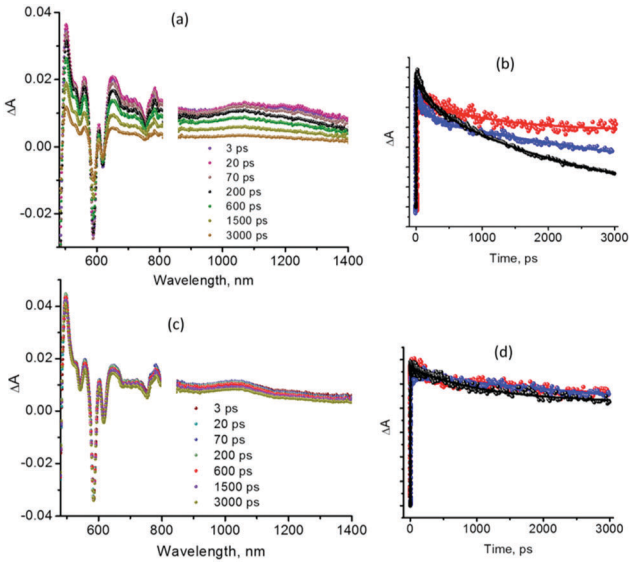

Fig. 6 Femtosecond transient absorption spectra of **WJ3** in (a) benzonitrile and (c) toluene at the indicated delay times. Figures (b) and (d) show the time profile of the near-IR peak corresponding to the singlet–singlet transition of **WJ3** (black), **WJ1** (red) and **WJ2** (blue), respectively, in benzonitrile and toluene.

profile of the singlet–singlet near-IR peak along with those of the other two porphyrin derivatives is shown in Fig. 6d. In contrast to the faster decay observed in benzonitrile, the decay of **WJ3** was slow and was similar to that of **WJ1** and **WJ2**, implicating little or no intramolecular charge transfer-type interactions in nonpolar toluene (see Fig. S5 for the transient spectra of **WJ1** and **WJ2** in toluene).

Finally, nanosecond transient spectra were recorded to characterize the triplet excited push–pull benzoporphyrins. Fig. 7a shows the nanosecond transient spectra of **WJ3** in Ar-saturated benzonitrile solution. The triplet excited **WJ3** displayed peaks at 505, 658, 705, and 830 nm similar to those of other free-base porphyrin derivatives reported in the literature.[28] The decay time constant for the 505 nm peak was 1.94 μs in benzonitrile (see the inset in Fig. 7a for the decay curve). Interestingly, this value was found to be nearly an order of magnitude smaller compared to those of **WJ1** and **WJ2**, being 85 μs and 80 μs in benzonitrile, respectively (see Fig. 7b and c for decay curves and Fig. S6 for the spectra, ESI†). Similar spectral features were also observed in toluene (see Fig. S6 in the ESI†). The decay time constants were found to be 7.02, 39.9 and 26.1 μs, respectively, for **WJ1**, **WJ2** and **WJ3**. In contrast to the trend observed in benzonitrile, the data in toluene lacked any specific trend. These results suggest the occurrence of push–pull effects, *i.e.*, intramolecular charge transfer-type interactions, arising from the excited triplet state of the free-base porphyrin in **WJ3** in polar benzonitrile.

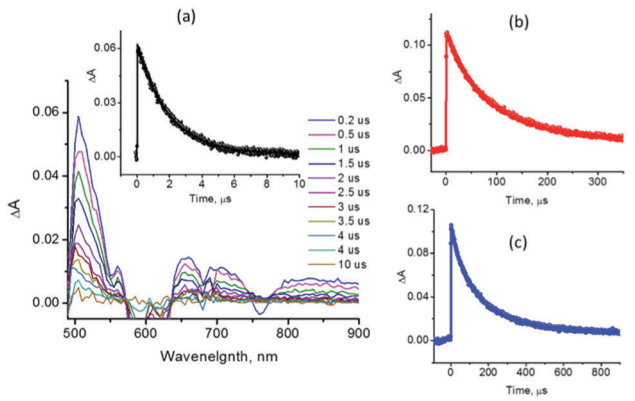

Fig. 7 (a) Nanosecond transient absorption spectra of **WJ3** in Ar-saturated benzonitrile at the indicated delay times (λ_{ex} = 466 nm, 7 ns pulses). The decay profile of the 505 nm peak is shown in the figure inset, while those of **WJ1** and **WJ2** are shown in figures (b) and (c), respectively.

Experimental

General

The chemicals used in the synthesis were obtained from Aldrich. All other chemicals used for the synthesis were of reagent grade unless otherwise specified. Column chromatography was performed on silica (60–120 mesh). The NMR spectra were recorded in $CDCl_3$ on a Bruker 500 MHz instrument. Tetramethylsilane [$Si(CH_3)_4$] was used as an internal standard. All samples were prepared in $CDCl_3$ or a $CDCl_3$/MeOD mixture and the chemical shifts were referenced to $CHCl_3$ at 7.26 ppm for ^1H NMR and to $CDCl_3$ at 77.0 ppm for ^{13}C NMR. Mass spectra were obtained on a Thermoscientific MALDI-LTQ-XL-Orbitrap mass spectrometer. The UV-visible spectral measurements were carried out using a Shimadzu Model 2550 double monochromator UV-visible spectrophotometer. The fluorescence emission was monitored by using a Horiba Yvon Nanolog coupled with time-correlated single photon counting with nanoLED excitation sources. A right angle detection method was used.

Synthesis of push–pull porphyrins

Porphyrins **1–5** were synthesized according to previously published procedures.[22]

General procedure for the synthesis of dibenzoporphyrins WJ1–WJ3

Dibromoporphyrin (1.00 eq.) and K_2CO_3 (2.20 eq.) were added to a Schlenk flask and dried under vacuum. The vacuum was released under argon to allow the addition of dry THF (20 mL). The mixture was then degassed *via* three freeze–pump–thaw cycles before the addition of $Pd[P(tBu)_3]_2$ (0.03 eq.) and an enyne (15 eq.). The Schlenk flask was then sealed and the reaction mixture was heated at 35 °C for 24 h. Then, the temperature of the reaction mixture was raised to reflux for 24 h. Then, the solvent was removed and redissolved in CH_2Cl_2 and washed with water. The organic layer was removed under vacuum. The resulting residue was subjected to silica column chromatography (CH_2Cl_2/MeOH). The band containing the desired porphyrin was collected and the porphyrin was recrystallized from CH_2Cl_2/MeOH.

WJ1. Brown solid, 14 mg, 0.010 mmol, 25%, (mp > 300 °C), UV-vis (toluene) λ_{max} (log ε) 452 nm (5.85), 533 (4.61), 570 (4.59), 612 (4.27), 668 (3.52). ^1H NMR (500 MHz, $CDCl_3$)

δ 9.02 (d, J = 4.9 Hz, 2H), 8.98 (d, J = 4.8 Hz, 2H), 8.16–7.92 (m, 12H), 7.62 (d, J = 6.6 Hz, 4H), 7.50–7.38 (m, 6H), 7.19 (s, 2H), 6.87 (s, 2H), 3.91 (s, 6H), 1.55 (s, 36H), 1.52 (s, 36H), −2.62 (s, 2H). ^{13}C NMR (126 MHz, $CDCl_3$) δ 168.54, 150.71, 150.44, 149.62, 148.30, 143.01, 141.21, 141.10, 141.01, 139.06, 138.72, 131.54, 129.05, 128.85, 128.40, 128.15, 128.02, 127.92, 127.87, 127.77, 125.71, 123.90, 122.60, 122.18, 122.08, 120.01, 119.65, 92.69, 89.78, 52.19, 35.23, 35.17, 31.75, 31.69. HRMS (MALDI) m/z: $[M]^+$ calcd for $C_{104}H_{110}N_4O_4$ 1478.8527; found 1478.8541.

WJ2. Brown solid, 12 mg, 0.008 mmol, 20%, (mp > 300 °C), UV-vis (toluene) λ_{max} (log ε) 459 nm (5.30), 534 (4.32), 573 (4.45), 613 (4.00), 670 (3.43). ^{1}H NMR (500 MHz, $CDCl_3$) δ 8.97 (br.s, 2H), 8.93 (br.s, 2H), 8.03 (br.s, 10H), 7.95 (s, 2H), 7.49 (d, J = 7.6 Hz, 4H), 7.16 (s, 2H), 6.76 (s, 2H), 6.75 (d, J = 10.7 Hz, 4H), 3.88 (s, 6H), 3.01 (s, 12H), 1.52 (S, 36H), 1.49 (s, 36H), −2.63 (s, 2H). ^{13}C NMR (126 MHz, $CDCl_3$) δ 168.72, 150.80, 150.51, 150.35, 150.11, 148.16, 143.09, 141.43, 141.24, 140.64, 139.26, 138.66, 132.89, 128.84, 128.60, 128.08, 128.02, 127.72, 125.81, 123.44, 122.22, 122.14, 120.01, 119.63, 112.05, 111.27, 94.13, 88.28, 52.30, 40.46, 35.36, 35.30, 31.92, 31.82. HRMS (MALDI) m/z: $[M]^+$ calcd for $C_{108}H_{120}N_6O_4$ 1564.9371; found 1564.9382.

WJ3. Brown solid, 22 mg, 0.014 mmol, 21%, (mp > 300 °C), UV-vis (toluene) λ_{max} (log ε) 466 nm (5.17), 542 (4.13), 584 (4.47), 617 (4.09), 674 (3.12). ^{1}H NMR (500 MHz, $CDCl_3$) δ 8.99 (m, 4H), 8.08 (d, J = 1.7 Hz, 4H), 8.03 (m, 8H), 7.54–7.44 (m, 8H), 7.40–7.33 (m, 1H), 7.27 (s, 2H), 6.76 (s, 2H), 6.75 (d, J = 8.8 Hz, 4H), 3.06 (s, 12H), 1.53 (s, 36H), 1.50 (s, 36H), −2.55 (s, 2H). ^{13}C NMR (126 MHz, $CDCl_3$) δ 167.38, 150.75, 150.71, 150.65, 150.01, 147.72, 145.67, 141.17, 140.88, 140.52, 139.63, 138.52, 132.77, 132.33, 129.04, 128.51, 128.46, 128.15, 128.05, 127.89, 127.71, 127.60, 126.59, 123.49, 122.56, 122.17, 120.57, 120.53, 119.50, 111.92, 111.07, 94.16, 88.11, 40.33, 35.24, 31.79, 31.71. HRMS (MALDI) m/z: $[M]^+$ calcd for $C_{112}H_{119}N_7O_2$ 1593.9425; found 1593.9452.

Instrumentation

Differential pulse and cyclic voltammograms were recorded on an EG&G 263A electrochemical analyzer using a three-electrode system. A platinum button electrode was used as the working electrode. A platinum wire served as the counter electrode and an Ag/AgCl electrode was used as the reference electrode. The ferrocene/ferrocenium redox couple was used as an internal standard. All the solutions were purged prior to electrochemical and spectral measurements using argon gas. Spectroelectrochemical studies were performed by using a cell assembly (SEC-C) supplied by ALS Co., Ltd (Tokyo, Japan). This assembly comprised of a Pt counter electrode, a 6 mm Pt gauze working electrode, and an Ag/AgCl reference electrode in a 1.0 mm path length quartz cell. The optical transmission was limited to 6 mm covering the Pt gauze working electrode.

Femtosecond pump–probe transient spectroscopy

Femtosecond transient absorption spectroscopy experiments were performed using an ultrafast femtosecond laser source (Libra) by coherently incorporating a diode-pumped, mode locked Ti:sapphire laser (Vitesse) and a diode-pumped intra cavity doubled Nd:YLF laser (Evolution) to generate a compressed laser output of 1.45 W. For optical detection, a Helios transient absorption spectrometer (Ultrafast Systems LLC) coupled with a femtosecond harmonic generator (Ultrafast Systems LLC) was used. The pump and probe pulses were derived from the fundamental output of the Libra ultrafast femtosecond laser source (compressed output 1.45 W, pulse width 100 fs) at a repetition rate of 1 kHz. 95% of the fundamental output of the laser was introduced into the harmonic generator, which produces second and third harmonics of 400 and 267 nm besides the fundamental 800 nm for excitation, while the rest of the output was used for the generation of white light continuum. In the present study, the second harmonic 400 nm excitation pump was used in all the experiments. Kinetic traces at appropriate wavelengths were assembled from the time-resolved spectral data. Data analysis was performed using the Surface Xplorer software supplied by Ultrafast Systems. All measurements were conducted in degassed solutions at 298 K.

Nanosecond laser flash photolysis

The studied compounds were excited by a Opolette HE 355 LD pumped by a high energy Nd:YAG laser with a second and third harmonic OPO (tuning range 410–2200 nm, pulse repetition rate 20 Hz, pulse length 7 ns) with powers of 1.0 to 3 mJ per pulse. The transient absorption measurements were performed using a Proteus UV-vis-NIR flash photolysis spectrometer (Ultrafast Systems, Sarasota, FL) with a fibre optic delivering white probe light and either a fast rise Si photodiode detector covering the 200–1000 nm range or an InGaAs photodiode detector covering the 900–1600 nm range. The output from the photodiodes and a photomultiplier tube was recorded using a digitizing Tektronix oscilloscope.

Conclusions

The newly synthesized π-extended, β-functionalized, push–pull dibenzoporphyrins bearing an ethynylphenyl spacer between the push (tertiary amine) groups and the benzoporphyrin core revealed several interesting properties. First, the existence of the electronic coupling between the push and the pull groups through the porphyrin π-system led to a considerable decrease in the HOMO–LUMO energy gaps. As a result, both the absorption and the emission peaks were red-shifted. Accordingly, facile electrochemical oxidation and reduction processes were observed. The calculated frontier orbitals revealed that the HOMO of both **WJ2** and **WJ3** was delocalized over the electron donating groups, while the LUMO of **WJ2** and **WJ3** was delocalized on the electron withdrawing groups. This significant orbital segregation observed for **WJ2** and **WJ3** can be attributed to the electron-donating amine groups in these two porphyrins. The lifetime of the singlet excited state and the steady-state fluorescence intensity of **WJ3** were reduced significantly relative to those of **WJ1** and **WJ2**. The successful formation of the singlet excited state in all these three push–pull benzoporphyrins was established from femtosecond transient absorption studies. As a consequence of intramolecular charge transfer-type interactions, relaxation of the singlet excited state was faster in **WJ3** compared to **WJ1** and **WJ2** in polar solvent

but not in nonpolar solvent. The presence of intramolecular charge transfer-type interactions from the triplet excited state of **WJ3** in benzonitrile was further confirmed by the results obtained from nanosecond transient absorption studies. The occurrence of intramolecular events originating from both singlet and triplet excited states of these push–pull benzoporphyrins is noteworthy in this work. Our studies suggest that **WJ3**, which carries two electron-donating amino groups and a strongly electron-withdrawing cyclic imide group, displays better push–pull effects compared to the other two push–pull benzoporphyrins, which carry weaker electron-donating (**WJ1**) or electron-withdrawing (**WJ2**) groups.

Acknowledgements

The authors are thankful to Dr David Hrovat and Dr Tom Cundari for helpful discussions. Support from the U.S. Department of Energy, Office of Science, Basic Energy Sciences (DE-FG02-13ER46976) and the National Science Foundation (grant no. 1401188 to FD) is acknowledged.

Notes and references

1 M. O. Senge, M. Fazekas, E. G. A. Notaras, W. J. Blau, M. Zawadzka, O. B. Locos and E. M. Ni Mhuircheartaigh, *Adv. Mater.*, 2007, **19**, 2737–2774.
2 G. Di Carlo, S. Caramori, V. Trifiletti, R. Giannuzzi, L. De Marco, M. Pizzotti, A. Orbelli Biroli, F. Tessore, R. Argazzi and C. A. Bignozzi, *ACS Appl. Mater. Interfaces*, 2014, **6**, 15841–15852.
3 T. Higashino and H. Imahori, *Dalton Trans.*, 2015, **44**, 448–463.
4 G. d. l. Torre, P. Vázquez, F. Agulló-López and T. Torres, *J. Mater. Chem. A*, 1998, **8**, 1671–1683.
5 A. Chaudhary, A. Srinivasan and T. K. Chandrashekar, *Handbook of Porphyrin Science*, 2014.
6 H. Imahori, T. Umeyama and S. Ito, *Acc. Chem. Res.*, 2009, **42**, 1809–1818.
7 M. Urbani, M. Gratzel, M. K. Nazeeruddin and T. Torres, *Chem. Rev.*, 2014, **114**, 12330–12396.
8 L. L. Li and E. W. Diau, *Chem. Soc. Rev.*, 2013, **42**, 291–304.
9 C. Y. Lin, C. F. Lo, L. Luo, H. P. Lu, C. S. Hung and E. W. G. Diau, *J. Phys. Chem. C*, 2009, **113**, 755–764.
10 A. Yella, H.-W. Lee, H. N. Tsao, C. Yi, A. K. Chandiran, M. K. Nazeeruddin, E. W.-G. Diau, C.-Y. Yeh, S. M. Zakeeruddin and M. Grätzel, *Science*, 2011, **334**, 629–634.
11 A. Yella, C. L. Mai, S. M. Zakeeruddin, S. N. Chang, C. H. Hsieh, C. Y. Yeh and M. Gratzel, *Angew. Chem., Int. Ed.*, 2014, **53**, 2973–2977.
12 S. Mathew, A. Yella, P. Gao, R. Humphry-Baker, B. F. Curchod, N. Ashari-Astani, I. Tavernelli, U. Rothlisberger, M. K. Nazeeruddin and M. Gratzel, *Nat. Chem.*, 2014, **6**, 242–247.
13 C.-L. Wang, J.-Y. Hu, C.-H. Wu, H.-H. Kuo, Y.-C. Chang, Z.-J. Lan, H.-P. Wu, E. Wei-Guang Diau and C.-Y. Lin, *Energy Environ. Sci.*, 2014, **7**, 1392.
14 J. P. Hill, *Angew. Chem., Int. Ed.*, 2016, **55**, 2976–2978.
15 I. Obraztsov, W. Kunter and F. D'Souza, in *Electrochemistry of N4 Macrocylic Metal Complexes*, ed. J. H. Zagal and F. Bedioui, Springer, Switzerland, 2016, vol. 1, pp. 171–262.
16 H. Hayashi, A. S. Touchy, Y. Kinjo, K. Kurotobi, Y. Toude, S. Ito, H. Saarenpaa, N. V. Tkachenko, H. Lemmetyinen and H. Imahori, *ChemSusChem*, 2013, **6**, 508–517.
17 J. Chen, K.-L. Li, Y. Guo, C. Liu, C.-C. Guo and Q.-Y. Chen, *RSC Adv.*, 2013, **3**, 8227–8231.
18 G. Di Carlo, A. Orbelli Biroli, M. Pizzotti, F. Tessore, V. Trifiletti, R. Ruffo, A. Abbotto, A. Amat, F. De Angelis and P. R. Mussini, *Chem. – Eur. J.*, 2013, **19**, 10723–10740.
19 R. Deshpande, L. Jiang, G. Schmidt, J. Rakovan, X. Wang, K. Wheeler and H. Wang, *Org. Lett.*, 2009, **11**, 4251–4253.
20 L. Jiang, J. T. Engle, L. Sirk, C. S. Hartley, C. J. Ziegler and H. Wang, *Org. Lett.*, 2011, **13**, 3020–3023.
21 H. L. Anderson, *Chem. Commun.*, 1999, 2323–2330.
22 R. G. Jinadasa, Y. Fang, S. Kumar, A. J. Osinski, X. Jiang, C. J. Ziegler, K. M. Kadish and H. Wang, *J. Org. Chem.*, 2015, **80**, 12076–12087.
23 M. J. Frisch, G. W. Trucks, H. B. Schlegel, G. E. Scuseria, M. A. Robb, J. R. Cheeseman, V. G. Zakrzewski, J. A. Montgomery, R. E. Stratmann, J. C. Burant, S. Dapprich, J. M. Millam, A. D. Daniels, K. N. Kudin, M. C. Strain, O. Farkas, J. Tomasi, V. Barone, M. Cossi, R. Cammi, B. Mennucci, C. Pomelli, C. Adamo, S. Clifford, J. Ochterski, G. A. Petersson, P. Y. Ayala, Q. Cui, K. Morokuma, D. K. Malick, A. D. Rabuck, K. Raghavachari, J. B. Foresman, J. Cioslowski, J. V. Ortiz, B. B. Stefanov, G. Liu, A. Liashenko, P. Piskorz, I. Komaromi, R. Gomperts, R. L. Martin, D. J. Fox, T. Keith, M. A. Al-Laham, C. Y. Peng, A. Nanayakkara, C. Gonzalez, M. Challacombe, P. M. W. Gill, B. G. Johnson, W. Chen, M. W. Wong, J. L. Andres, M. Head-Gordon, E. S. Replogle and J. A. Pople, *GAUSSIAN 03*, Gaussian, Inc., Pittsburgh PA, 2003.
24 K. M. Kadish, *Prog. Inorg. Chem.*, 1986, **34**, 435–605.
25 G. N. Lim, W. A. Webre and F. D'Souza, *J. Porphyrins Phthalocyanines*, 2015, **19**, 270–280.
26 G. N. Lim, E. Maligaspe, M. E. Zandler and F. D'Souza, *Chem. – Eur. J.*, 2014, **20**, 17089–17099.
27 P. K. Poddutoori, G. N. Lim, A. S. D. Sandanayaka, P. A. Karr, O. Ito, F. D'Souza, M. Pilkington and A. van der Est, *Nanoscale*, 2015, **7**, 12151–12165.
28 N. M. B. Neto, D. S. Correa, L. De Boni, G. G. Parra, L. Misoguti, C. R. Mendonca, I. E. Borissevitch, S. C. Zilio and P. J. Goncalves, *Chem. Phys. Lett.*, 2013, **587**, 118–123.

